RSC Advances

ROYAL SOCIETY OF CHEMISTRY

www.rsc.org/advances

A WAXS/SAXS Study on the Deformation Behavior of β – nucleated Propylene – Ethylene Random Copolymer Subjected to Uniaxial Stretching

Chunbo Zhang, Guoming Liu*, Qianhong Jiang, Jian Yang, Ying Zhao*, Dujin Wang

Beijing National Laboratory for Molecular Sciences, CAS Key Laboratory of Engineering Plastics, Institute of Chemistry, Chinese Academy of Sciences, Beijing, 100190, China

Copolymerization for making propylene – based random copolymers is an important strategy to broaden the applications of polypropylene, such as propylene random copolymer with β – nucleating agent as hot water pipes. In the present work, a β – nucleated propylene – ethylene random copolymer (P – E copolymer) containing a low content of ethylene (5.6 mol %) was subjected to uniaxial stretching at 30 and 100 °C. The structural evolution during deformation was investigated by *in – situ* X – ray scattering using synchrotron radiation. An interesting temperature dependence of the deformation feature of β – crystal was observed. The β – crystal in the sample transformed to mesophase at 30 °C and to α – crystal at 100 °C. Molecular chains in β – crystal stretched at 30 °C was identified to be perpendicular to the stretching direction, while they tended to be parallel to the direction at 100 °C. On the other hand, cavitation was observed in β – nucleated P – E copolymer when stretched at 30 °C. As the tensile temperature reached 100 °C, no cavities could be detected. A deformation model of the β – nucleated P – E copolymer combining crystal transition, cavitation and orientation depending on the drawing temperature was described.

Introduction

As a most fundamental way in altering the chemical or physical properties, copolymerization essentially contributes to the diversity and versatility of polymer materials. Especially for polyolefin, copolymerization of comonomers has achieved great industrial success, as the properties of copolymers can be tuned by the comonomer type, content, and sequence distribution. [1-6] Among olefin copolymers, random copolymer of propylene is one type of propylene-based copolymers prepared via Ziegler-Natta [7,8] or metallocene catalysts [3,5].

The most commonly used comonomer in propylene random copolymers is ethylene. Ethylene units are partially included in the polypropylene crystalline phase, which has been proven by the ^{13}C

– NMR and X – ray diffraction. [8-10] It should be noted that the dimension of the crystal lattice are not largely affected.[10,11] Incorporation with certain amount of ethylene units (1 – 30 mol%)[3,12,13], propylene – ethylene random copolymers (P – E copolymers) have the same polymorphism as isotactic polypropylene (iPP), i.e. the α –, β – and γ – form crystals and mesophase [14-1819] can be obtained under certain conditions. However, the crystallization behaviors[2,3] are quite different. The introduction of ethylene units leads to decreased melting and crystallization temperatures, and lower crystallinities.[12,13] The mechanical properties of P – E copolymers vary from thermoplastic to elastomeric over the range of ethylene content from 3 mol % to 30 mol %.[13]

P – E copolymers with low contents of ethylene (1-10 wt %) [20,21] are usually used as structural materials, so it is important to understand their behaviors under mechanical load. Deformation mechanism of iPP has been studied extensively in literatures. [22-24] Tensile deformation process of iPP is often accompanied with orientation, crystal transition and cavitation, all of which are temperature dependent. The α – crystal in iPP has a *c* – axis orientation at elevated temperature[25,26], and transforms to mesophase with polymer chains parallel to the stretching direction at room temperature[27,28]. The β – crystal in iPP is unstable during deformation and transforms either to mesophase or to α – crystal depending on deformation temperature. [29-33] The cavitation in iPP becomes less prominent when the stretching temperature increases and finally disappears. [34-37] P – E copolymers with low contents of ethylene have similar stress – strain behavior with iPP[13,38,39], exhibiting typical characteristics of semicrytalline polymer. However, the presence of ethylene units leads to the decrease of yield stress and modulus[13].

Adding β – nucleating agent to P – E copolymers with low contents of ethylene has been proven to improve their impact toughness[40,41]. However, the disturbance of regularity of polymer chain in P – E copolymers highly reduced the tendency to form β – crystal[14,15]. The deformation process of P – E copolymers containing predominately β – crystal has not been reported in literature. In addition, the randomly incorporated comonomers result in a lower glass transition temperature and a lower melting point, which makes it easier to investigate the influence of temperature on the deformation of β – crystal. In this work, calcium pimelate, a selective β – nucleating agent was used for P – E copolymer to crystallize predominately in β – crystal. The uniaxial tensile deformation of β – nucleated P – E copolymer was investigated by *in – situ* small – angle and wide – angle X – ray scattering (SAXS/WAXS) at different temperatures (30 and 100 ºC), aiming to understand the influence of drawing temperature on the changes of polymorphism, cavitation and preferred

orientation.

Experimental

Materials

The P – E copolymer prepared via Ziegler-Natta catalyst was supplied by SINOPEC Beijing Yanshan Company. The number – average molecular weight (M_n) was 163000 g/mol, and the polydispersity index was 3.54. The mole fraction of ethylene unit was about 5.6 %. Calcium pimelate (Ca – Pim), a β – nucleating agent, was synthesized in our laboratory [42].

Sample preparation

P – E copolymer and Ca – Pim powders were blended in a mixer (HAAKE Rheomix OS) at 200 °C for 6 min with a rotating speed of 50 rpm.The fraction of β – nucleating agent was 0.1 wt %. The obtained mixture was hot – pressed at 210 °C to obtain plaques with thickness about 1 mm. The samples were melted at 210 °C for 5 min and then cooled to 115 °C for isothermal crystallization on a Linkam LTS350 hotstage (Linkam Scientific Instruments, Ltd., U.K.). After annealing for 60 min, the plaques were cooled at 30 °C/min to room temperature. Mini tensile bars were cut from the plaques.

Differential scanning calorimetry (DSC)

The melting behavior of the undeformed sample was examined with a TA instruments DSC Q2000. The instrument was calibrated with indium before measurements. Temperature scans were performed at a heating rate of 10 °C/min under protection of nitrogen atmosphere.

Dynamic mechanical analysis (DMA)

Dynamic mechanical analysis (DMA) was carried out using a DMA Q800 analyzer (TA instruments, USA). Rectangular shaped samples were measured in tension mode from −100 to 120 °C at a heating rate of 3 °C/min and frequency of 1 Hz. The strain was set to be 0.05%.

Scanning electron microscope (SEM)

The morphology of β – nucleated P – E copolymer was observed on a JSM – 6700 JEOL SEM, operated at an accelerating voltage of 5 kV. The sample was gold sputtered prior to the SEM observation.

In – situ Synchrotron X – ray measurements

In – situ X – ray measurements were carried out at the beamline BL16B1 in the Shanghai Synchrotron Radiation Facility (SSRF). The wavelength of the radiation source was 1.24 Å. The samples were stretched on a Linkam TST 350 tensile hotstage at 30 and 100 °C, respectively. Once the temperature reached the desired value at a rate of 30 °C/min, the sample was equilibrated for 2 min and then stretched with jaws moving symmetrically at a constant speed of 3.0 mm/min. The structural information was recorded by WAXS and SAXS in a time – resolved manner. All scattering patterns were captured *in – situ* by a MAR CCD (MAR–USA) detector with a resolution of 2048 × 2048 pixels and pixel size of 79 × 79 μm^2. Pattern acquisition time was 15 s for WAXS, and the sample to detector distance was 194 mm. Pattern acquisition time for SAXS was 1 s and 30 s at 30 and 100 °C, respectively. The sample to detector distance for SAXS was 5210 mm. Air scattering was subtracted from the experimental data in all data analysis.

Results and discussion

Initial structure of the undeformed β – nucleated P – E copolymer

The WAXS pattern of the undeformed β – nucleated P – E copolymer is shown in Figure 1a. All three crystal modifications of iPP can be observed. The two strongest diffraction peaks can be indexed as the 110_β and $111_\beta/111_\alpha$, respectively. This reveals that the β – form is predominant in the initial sample. According to characterizing parameter proposed by Turner-Jones et al. [43], k_β, the ratio of the strong single β – crystal peak and the sum of the strongest reflections, is 0.74, which is a high value for β – nucleated P – E copolymers. Evidently, the reflection rings are uniform in 2D scattering patterns, indicating that the distribution of the β crystallites is random. SEM micrograph in Figure 1b also shows that the undeformed β – nucleated P – E copolymer contains β – crystal spherulite exhibiting bundle – like radial lamellar arrangement. The isotropy of initial sample provides a basis for orientation analysis of β – crystal in β – nucleated P – E copolymer during stretching. The characteristic reflections of α modification consist of 110_α, 040_α, 130_α, and 111_α planes with *d* – spacing of 6.25, 5.18, 4.76 and 4.16 Å, respectively. While for γ form it consists of reflections from 111_γ, 008_γ and 117_γ planes with *d* – spacing of 6.40, 5.30 and 4.42 Å, respectively. Due to the various line broadening mechanism, the peaks of α and γ forms usually overlap, except for the 130_α reflection for α – crystal and 117_γ reflection for γ – crystal.

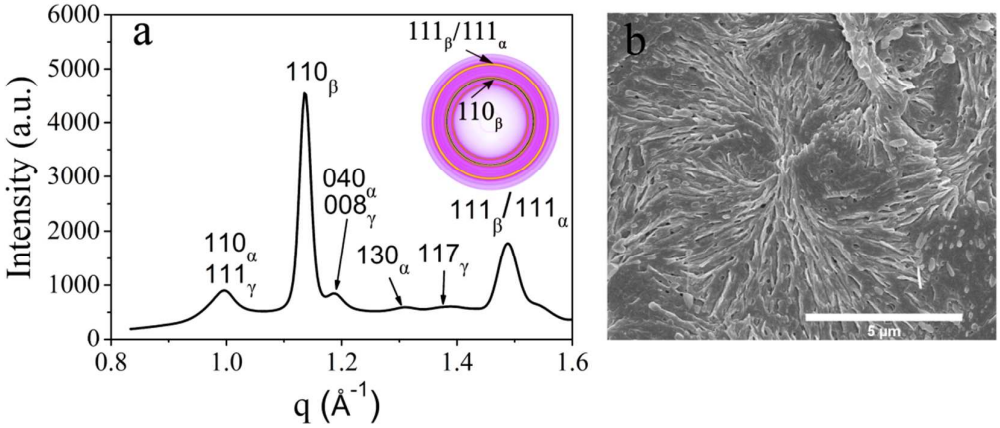

FIGURE 1 Undeformed β – nucleated P – E copolymer: (a) indexed 1D WAXS intensity profile at room temperature (inset shows 2D pattern). The scattering vector is defined as $q = 4\pi\times\sin\theta/\lambda$, in which θ is the half Bragg angle, λ is the wavelength of the radiation. (b) The SEM micrograph of etched cyro – fractured surface of the undeformed β – nucleated P – E copolymer.

The DSC heating trace for the undeformed β – nucleated P – E copolymer is shown in Figure 2. The thermal behavior of P – E copolymer without β – nucleating agent is also presented for comparison purpose. The β – nucleated P – E copolymer exhibits two distinct melting peaks located at 129.1 and 145.6 °C, respectively. The peaks are attributed to the melting of β and α – form crystals, respectively. The partial disturbance of chain regularity by the randomly incorporated ethylene units results in a reduced thickness of lamellae [11]. Therefore, the melting points of α and β crystals in P – E copolymer are lower than those in homopolypropylene. It should be noticed that the melting temperature of α – crystal in β – nucleated P – E copolymer is higher than that in P – E copolymer without β –nucleating agent. The increase of melting point results from the melting – recrystallization of β – crystal [44] during heating trace. Another shoulder peak at low temperature in the DSC curve may be related with γ – crystal [45]. The presence of γ – crystal can also be confirmed by the result of WAXS in Fig. 1a.

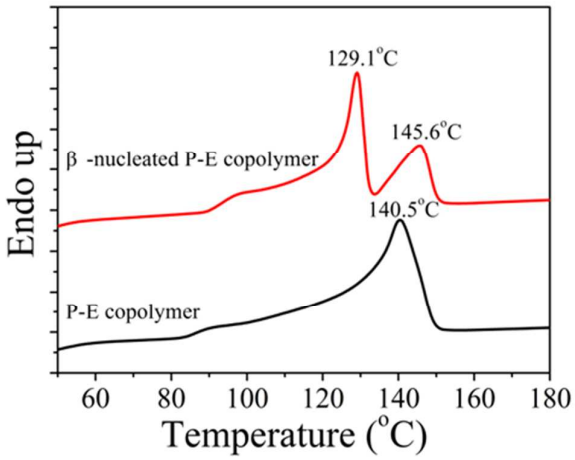

FIGURE 2 DSC melting traces for P – E copolymers with and without β – nucleating agent. The heating rate is 10°C/min.

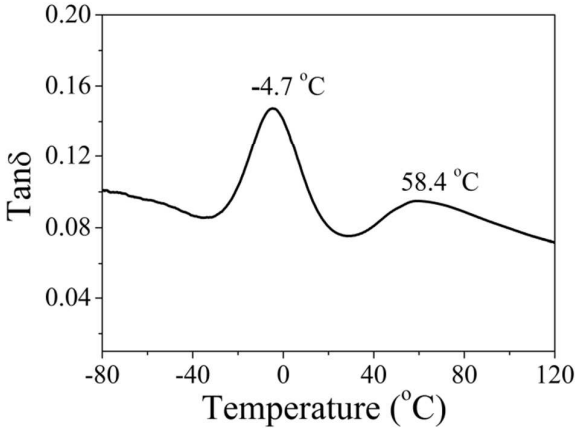

FIGURE 3 Mechanical loss factor (Tan δ) as a function of temperature for β – nucleated P – E copolymer.

Figure 3 shows the DMA curve for the β – nucleated P – E copolymer. The mechanical loss factor (Tan δ) curve is thought to be useful to characterize the microstructural change over a wide range of temperatures. The maximum at low temperature –4.7 °C is related to β relaxation, originating from the glass transition of the unrestricted amorphous phase (T_g). Due to the incorporation of ethylene, the T_g of P – E copolymer is lower than that of iPP. The peak at the higher temperature 58.4 °C represents α_c – relaxation, which is associated with the polymer chains rearrangements. It is assumed to originate from the helical jumps and chain diffusion through the crystallites [46].

Stress – strain curves of β – nucleated P – E copolymer at different temperatures

Figure 4 shows the engineering stress – strain curves obtained from tensile tests. The β – nucleated P – E copolymer exhibits typical ductile behavior with obvious elastic stage, yielding,

strain softening and strain hardening. The yield stress decreases from 19.5 to 4.5 MPa when the stretching temperature increases from 30 to 100 °C. It should be noted that the strain hardening behavior of β – nucleated P – E copolymer stretched at 100 °C is more obvious than that at 30 °C. The different mechanical response of sample at different temperatures may be due to different structural evolution during stretching, which will be further discussed in the following sections.

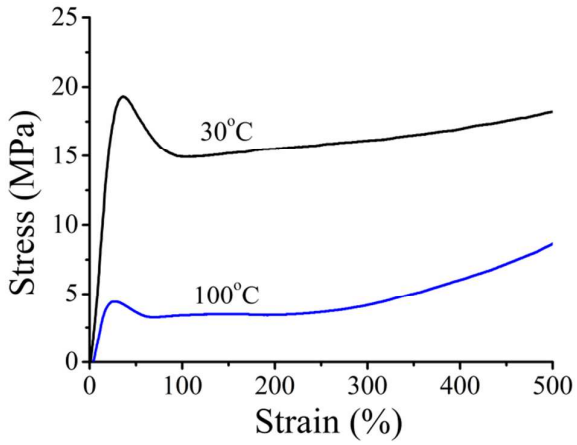

FIGURE 4 Engineering stress – strain curves of β – nucleated P – E copolymer at different temperatures. The stretching temperature is shown for each curve.

In – situ WAXS of β – nucleated P – E copolymer under stretching

Figure 5 presents the selected 2D WAXS patterns of β – nucleated P – E copolymer under tensile deformation at 30 and 100 °C. The corresponding 1D intensity profiles are shown in Figure 6. Combining Figure 5 and Figure 6, it can be concluded that α, β and γ modifications in β – nucleated P – E copolymer gradually transform to mesophase during stretching at 30 °C, while the β and γ forms transform to α phase at 100 °C. The overall feature of the crystal transition is similar to the β – nucleated iPP [30,33,47]. The final content of β – crystal in deformed P – E copolymer also depends strongly on stretching temperature. At 30 °C, a big amount of β – crystal still remains at strain = 450%. In contrast, the reflection of β – crystal cannot be observed when stretched at 100 °C.

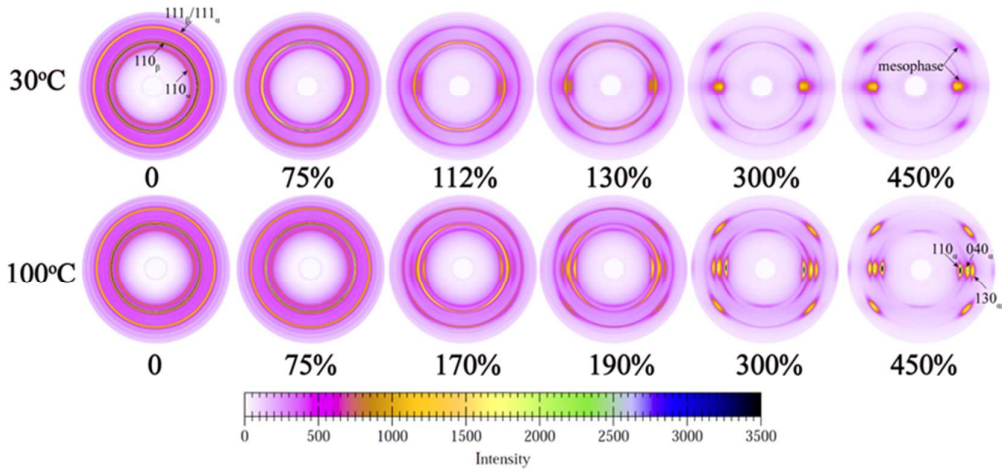

FIGURE 5 Selected WAXS patterns of β – nucleated P – E copolymer during tensile deformation at different temperatures. The drawing direction is vertical.

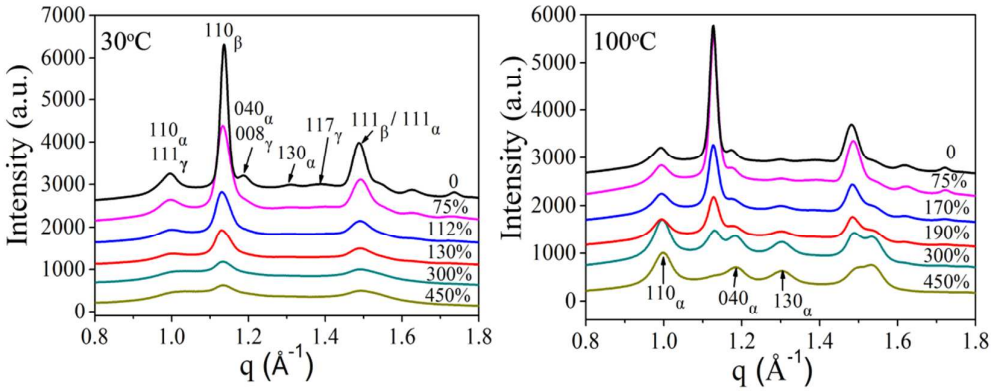

FIGURE 6 1D intensity profiles obtained from circularly integrated intensities (from 0 to 360°) of 2D WAXS patterns of β – nucleated P – E copolymer as a function of strain at different temperatures.

As the strain increased, the reflection rings become less uniform, indicating the orientation of crystallites occurs during deformation. In order to further characterize the orientation of β – crystal in β – nucleated P – E copolymer during stretching. The azimuthal distribution of 110_β reflection stretched at different temperatures is presented in Figure 7. Upon deformation, the orientation behaviors of β – crystal at tensile temperature of 30 °C are similar to those in β – iPP [42]. That is to say, the β – crystal in β – nucleated P – E copolymer displays an orientation with molecular chains perpendicular to the tensile direction when stretched at 30 °C. However, the orientation of 110_β reflection at 100 °C is obviously different (as shown in Figure 7) from 30 °C. At strain = 75 %, the intensity on the equator decreases. As the strain increased to 170 %, the ring becomes into four – arc – like diffractions concentrated at off – axis and the peak maxima are close to the equator. The 2D WAXS pattern in Figure 7 also indicates the orientation of α – crystal at 100 °C as the strain

increased. At strain = 190 %, the appearance of three equatorial arcs indexed as 110_α, 040_α, 130_α confirms the orientation. It should be noted that the 110_α arcs also occur on the meridian. This has been reported to be related to the parent – daughter lamellae structure in α – crystal [48]. And the orientation mode of α – crystal in mother lamellae can be determined as *c*–axis parallel to the stretching direction, while the *c*–axis in daughter lamellae has an 80° angle with respect to the fiber axis [49,50].

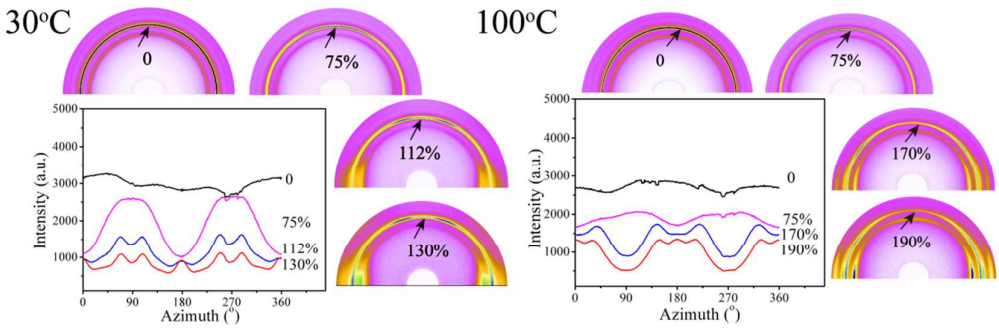

FIGURE 7 Azimuthal intensity distribution of 110_β (indicated by the arrows) of β – nucleated P – E copolymer as a function of strain at 30 and100 °C. The drawing direction is vertical.

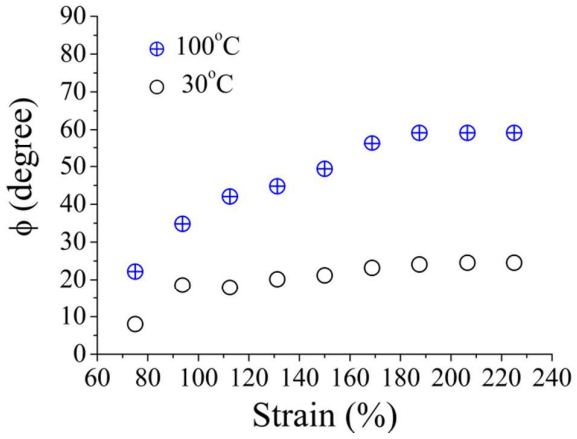

FIGURE 8 The angle between the normal of 110_β and the stretching direction during deformation of β – nucleated P – E copolymer at different temperatures.

Figure 8 depicts the change of angle between the normal of 110_β and the stretching direction during deformation at different temperatures. It should be mentioned that two equatorial peaks can be clearly observed at both 30 and 100 °C at large strains, which is not shown in the figure. The angle almost keeps constant under stretching at 30 °C, and the value is small. When β – nucleated P – E copolymer is stretched at 100 °C, the angle increases with strain increasing and levels off when the strain reaches 190%. The normal of 110_β tends to rotate to the equator direction, i.e. the

molecular chains tend to be aligned along the stretching direction during deformation. This orientation behavior of β – crystal with molecular chains parallel to the fiber axis has not been observed in β – iPP stretched at elevated temperatures, which may due to the rapid crystal transition from β to α – crystal.

In – situ SAXS of β – nucleated P – E copolymer under stretching

In – situ SAXS measurement can give more information on the change of lamellae during deformation. Figure 9 presents the selected SAXS patterns of β – nucleated P – E copolymer at different temperatures during tensile deformation. In the undeformed state, the samples show relatively weak but isotropic scattering ring, corresponding to uniform distribution of lamellar normal. The scattering intensity has an obvious increase at strain = 20% stretched at 30 °C, implying the occurrence of cavitation[35,36,51]. The intensity on the meridian is stronger than that on the equator, indicating that the cavities are elongated perpendicularly to the drawing direction. When strain = 50 %, the intensities on the meridian and equator become comparable. As strain further increased, the scattering intensity on the equator increases, while the intensity on the meridian decreases. It means that the reorientation of cavities occurs and at higher strains the cavities are preferentially elongated along the stretching direction. The cavities and their orientations can be observed by SEM. As shown in Figure10, the number of cavities increases with the engineering strain and the aspect ratio of cavities at strain = 50 % is smaller than those at strain = 200%. Upon temperature further increasing to 100 °C, no cavity signal can be detected in the β – nucleated P – E copolymer during stretching, but the isotropic scattering ring becomes non–uniform and the SAXS pattern changes gradually. The pattern changes from two – arc to four – arc pattern then to four – point pattern, indicating the tilting of lamellae in the sample during deformation. There are even six – point pattern appearing at strain = 190%, in agreement with the result of WAXS pattern displaying six arcs at strain = 190% (as showed in Figure 7). With strain further increasing, the pattern gradually evolves into two – point, demonstrating that the lamellar normals are parallel to the loading direction.

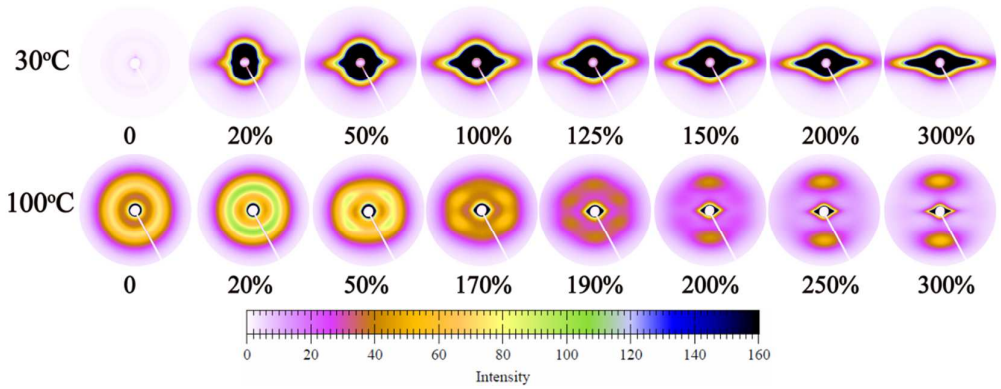

FIGURE 9 SAXS patterns of β – nucleated P – E copolymer stretched at different temperatures. The drawing direction is vertical.

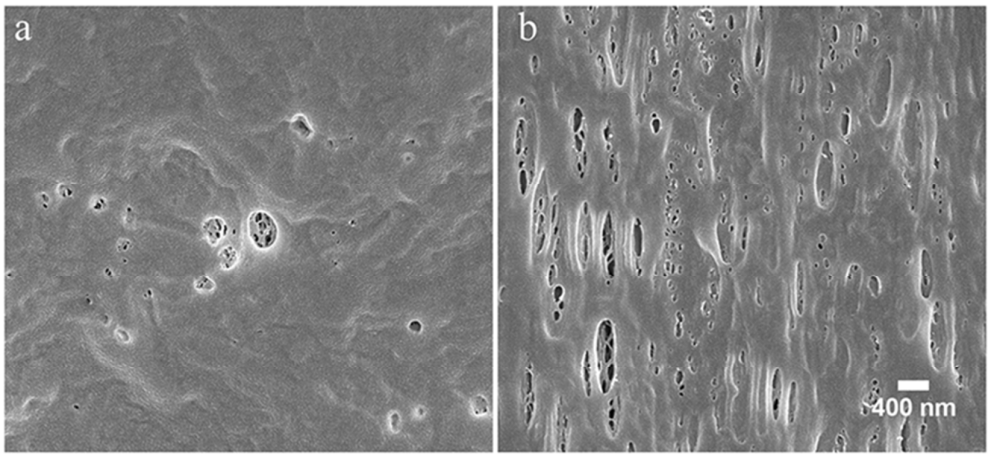

FIGURE 10 SEM images of β – nucleated P – E copolymer stretched at 30°C: (a) strain = 50 % and (b) strain = 200 %. The stretching direction is vertical.

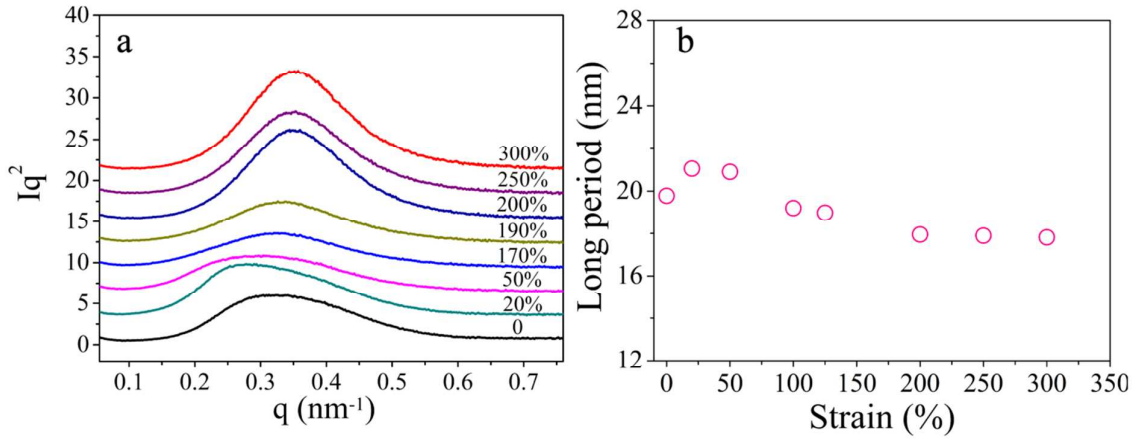

FIGURE 11 (a) Lorentz corrected 1D SAXS profiles of deformed β – nucleated P – E copolymer along the meridian at 100 °C. *q* is the scattering vector. (b) The long periods as a function of strain along the meridian.

The long period scattering may be covered by the scattering of cavities for the sample stretched at

30 °C. Nevertheless, the long period scattering is always visible during stretching at 100 °C. Figure 11 presents the 1D SAXS meridional profiles and long periods as a function of strain at 100 °C. It has been known that the long period can be estimated by $L = 2\pi/q_{max}$, in which q_{max} is the q value at the peak maximum [52]. A broad diffraction peak with $q_{max} = 0.32$ nm^{-1}, is observed in the undeformed sample. According to Figure 6, the β – form still is the dominating phase at the highest strain shown in Figure 11. Therefore the variation trend of long period is mainly related to the structural change of β – crystal. The long period increases from 19.6 nm at undeformed state to 21.1 nm at strain = 20 %, which is associated with the interlamellar separation under stretching. Upon further stretching, the long period decreases on account of the stress-induced melting and recrystallization[53,54], producing an oriented structure. Due to the low temperature, the thickness of lamellae formed during recrystallization at large strains is thinner than the initial lamellae.

Deformation processes of β – nucleated P – E copolymer at different temperatures

The above results indicate that the deformation of the β – nucleated P – E copolymer shares similar regulations with β – nucleated iPP. Meanwhile, the orientation of the β – crystal displays quite different features. The relation among crystal transition, orientation and cavitation during deformation of β – nucleated P – E copolymer and the influence of stretching temperature on these aspects are discussed as follows.

When stretching at 30 °C, cavitation takes place in β – nucleated P – E copolymer at strain = 20 %. At the beginning, cavities are oriented perpendicularly to the tensile direction. Subsequently, the reorientation of cavities occurs with strain increasing, i.e., the cavities are oriented along the stretching direction at high strains. Accompanying with the formation of cavities, the crystal transition from β to mesophase is observed after yielding, which may be achieved by melting and recrystallization mechanism [29]. The lamellae with chain direction parallel to the drawing direction are prone to be consumed by transforming to mesophase [47]. Thus the intensity of 110_β on the equator becomes weaker than that on the meridian. As pointed out in our previous work [42], the cavities release the local stress around the voids, providing "rooms" for the survival of the residual β – crystal blocks with chains perpendicular to the stretching direction.

With the increasing of stretching temperature from 30 to 100 °C, no cavitation occurs. The change of lamellar normal and the long period could be observed during deformation. The lamellar stacks are randomly oriented in the initial sample. At the initial stage of deformation, the increase of

long period corresponds to the interlamellar separation. After yielding, the crystals start to break up, the lamellae tend to tilt. The metastable β – crystal begins to transform to α – crystal, leading to the decrease of the fraction of lamellae with chain direction parallel to the drawing direction. As the deformation proceeds, lamellae undergo rotation and their normals are observed to be along the stretching direction, owing to higher chain mobility at this temperature.

The tensile temperature is expected to be crucial for the deformation of β – nucleated P – E copolymer, since cavitation, crystal orientation and transition are temperature dependent. A model of the deformation process is presented in Figure 12, which just focuses on the structural evolution of the lamellae with normal perpendicular to the drawing direction. For β – nucleated P – E copolymer, with the increase of stretching temperature, two modes of cavitation proposed by Wang et al. [55] are observed, namely "cavitation with reorientation" for the sample stretched at 30 ℃ and "no cavitation" at 100 °C. In fact, many factors influence cavitation in semicrystalline polymers, such as orientation, lamellar thickness[34,56], molecular weight stretching temperature and strain rate [35,57]. In this work, samples with the same molecular weight and lamellar thickness are used; therefore the drawing temperature and orientation are the critical factors. Indeed, shear yielding and cavitation have been identified as two major processes when a semicrystalline polymer is stretched. [34,58] Clearly, the stretching temperature has an effect on the sequence of cavitation and shear yielding occurring in β – nucleated P – E copolymer. Stretched at 30 ℃, the chain mobility is so poor that cavitation takes place before shear yielding. As shown in Figure 3, 100 °C is above the α_c – relaxation temperature of β – nucleated P – E copolymer, the helical jumps and chain diffusion through the crystallites are activated [46] and shear yielding of crystallites occurs instead of cavitation. This is confirmed by the SAXS result that no signal of cavities could be detected while signal from lamellar orientation could be observed when stretched at 100 ℃. The stress transfer by tie molecules [59-61] anchored in adjacent lamellae from loose to taut ones is also more effective at high temperature. Therefore the strain hardening behavior of β – nucleated P – E copolymer at 100 ℃ is more obvious than 30 °C (shown in Figure 4). On the other hand, the presence of ethylene units improves the mobility of P – E copolymer chains, the enhanced chain mobility and effective stress transfer make the lamellar blocks easy to rotate to their favorable orientation with chains parallel to the drawing direction. Thus the orientation behavior of β – crystal at 100 ℃ is different from that 30 ℃. The crystal transition is also affected by the stretching temperature. In our case, the β – mesophase and β – α transition are observed at 30 ℃ 100 ℃, respectively. This is consistent with

previous report [62] which showed that the stability up limit for mesophase in PP is 60 °C. In addition, the final content of β – crystal in β – nucleated P – E copolymer before fracture decreased with drawing temperature increasing.

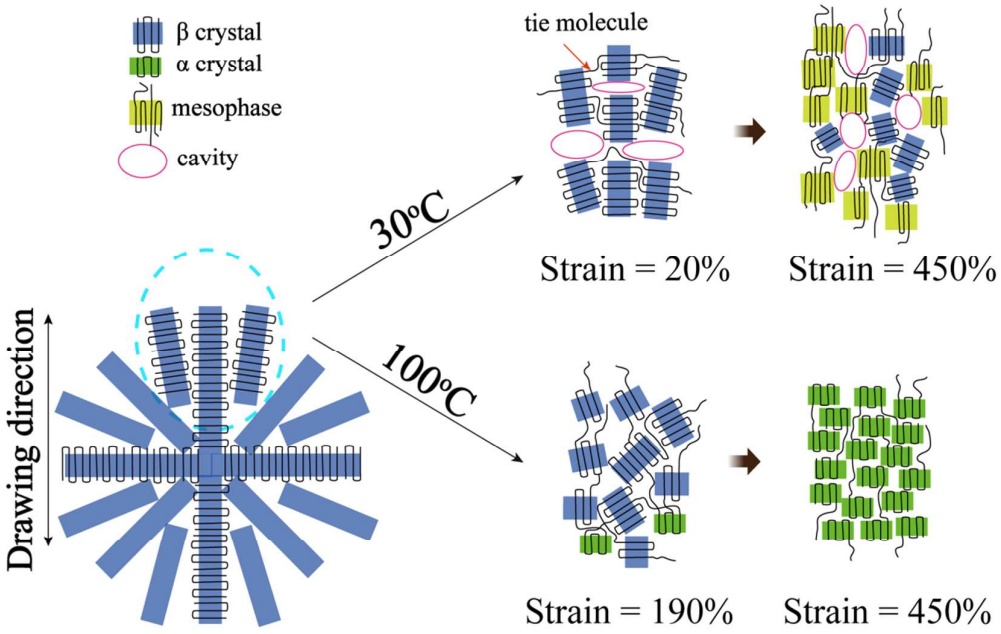

FIGURE 12 Schematic illustration of the deformation process of β – crystal in β – nucleated P – E copolymer during uniaxial stretching at different temperatures. This model just focuses on structural evolution of the lamellae with normal perpendicular to the drawing direction. The corresponding strains are shown in the diagram. (The ethylene co-units are not presented due to their low content).

Conclusions

The uniaxial tensile deformation process of initially isotropic β – nucleated P – E copolymer at different temperatures was studied by *in – situ* X – ray scattering. The crystal transition, cavitation and orientation couple with each other and affect the overall deformation process. The influence of stretching temperature on these aspects was investigated. The β – mesophase transition takes place at 30 °C, while β – α transition occurs at 100 °C. On the other hand, cavitation is observed in β – nucleated P – E copolymer when stretched at 30 °C. As the stretching temperature reaches 100 °C, no cavity signal can be detected. The crystal transition causes an orientation of β – crystal with molecular chains preferentially perpendicular to the stretching direction at 30 °C. But the β – crystal in β – nucleated P – E copolymer stretched at 100 °C displays different orientation behavior at middle strain. 100 °C is above the α_c – relaxation temperature of β – nucleated P – E copolymer, at

which the crystals become weaker and more disposed to shear. The high chain mobility and effective stress transfer make the lamellar blocks easy to rotate to their favorable orientation with chains parallel to the drawing direction.

Acknowledgements

Financial support from the National Natural Science Foundation of China (NSFC, Grant No. 51203170) is gratefully acknowledged. The SSRF is acknowledged for kindly providing the beam time.

Notes and references

1. I. L. Hosier; R. G. Alamo; P. Esteso; J. R. Isasi; L. Mandelkern. Macromolecules 2003, 36, 5623-5636.
2. K. Jeon; H. Palza; R. Quijada; R. G. Alamo. Polymer 2009, 50, 832-844.
3. C. D. Rosa; F. Auriemma; G. Talarico; O. R. Ballesteros; D. D. Luca; L. Resconi I. Camurati. Macromolecules 2007, 40, 6600-6616.
4. C. D. Rosa; F. Auriemma; G. Talarico; O. R. Ballesteros. Macromolecules 2007, 40, 8531-8532.
5. C. D. Rosa; F. Auriemma; G. Talarico; O. R. Ballesteros; D. D. Luca; L. Resconi. Macromolecules 2008, 41, 2172-2177.
6. X. W. Li; Y. M. Mao; C. Burger; Justin Che; B. S. Hsiao; R. R. Kulkarni; A. H. Tsou. *Polymer* **2013**, 54, 4545-4554.
7. R. Hingmann; J. Rieger; M. Kersting. *Macromolecules* **1995**, 28, 3801-3806.
8. S. Laihonen; U. W. Gedde; P. E. Werner; M. Westdahl; P. Jääskeläinen; J. Martinez-Salazar. *Polymer* **1997**, 38, 371-377.
9. R. G. Alamo; D. L. VanderHart; M. R. Nyden; L. Mandelkern. *Macromolecules* **2000**, 33, 6094-6105.
10. S. Hosoda; H. Hori; K. I. Yada; S. Y. Nakahara; M. Tsuji. *Polymer* **2002**, 43, 7451-7460.
11. D. Mileva; R. Androsch; H.J. Radusch. *Poly Bull* **2008**, 61, 643-654.
12. K. Jeon; Y. L. Chiari; R. G. Alamo. *Macromolecules* **2008**, 41, 95-108.
13. C. H. Stephens; B. C. Poon; P. Ansems; S. P. Chum; A. Hiltner; E. Baer. *J Appl Polym Sci* **2006**, 100, 1651-1658.
14. J. Varga; E. Schulek-Tóth. *J Therm Anal* **1996**, 47.
15. P. Juhasz; J. Varga; K. Belina; G. Belina. *J Macromol Sci B* **2002**, B41, 1173-1189.
16. D. R. Ferro; S. V. Meille; S. Briuckner; A J. Lovinger, F.J. Padden. *Macromolecules* **1994**, 27, 2615-2622.
17. D. L. Dorset; M. P. McCourt; S. Kopp; M. Schumacher; T. Okihara; B. Lotz. *Polymer* **1998**, 39, 6331-6337.
18. S.V. Meille; S. Bruckner. *Nature* **1989**, 340, 455-457.
19. D. Cavallo; F. Azzurri; R. Floris; G. C. Alfonso; L. Balzano; G. W. Peters. *Macromolecules* **2010**, 43, 2890-2896.
20. P. Jääskeläinen; J. Fiebig; M. Gahleitner; B. Malm; T. Schedenig. *EP 2042552A1*, 2009.
21. G. Hallot; J.M.R.G. Vion. US 2014000537A1, 2014.
22. A. Peterlin; F. J. Baltá‐Calleja. *J Appl Phys* **1969**, 40, 4238-4242.
23. A. Peterlin. *J Mater Sci* **1971**, 6, 490-508.
24. P. B. Bowden; R. J. Young. *J Mater Sci* **1974**, 9, 2034-2051.
25. G. M. Liu; X. Q. Zhang; Y. F. Liu; X. H. Li; H. Y. Chen; K. Walton; G. Marchand; D. J. Wang. *Polymer* **2013**, 54, 1440-1447.
26. J. Martin; M. Ponçot; J. M. Hiver; P. Bourson; A. Dahoun. *J Raman Spectrosc* **2013**, 44, 776-784.
27. R. F. Saraf; R. S. Porter. *Polym Eng Sci* **1988**, 28, 842-851.

28. S. Osawa; R. S. Porter. *Polymer* **1994**, 35, 545-550.
29. J. X. Li; W. L. Cheung. *Polymer* **1998**, 39, 6935-6940.
30. Z. W. Cai; Y. Zhang; J. Q. Li; F. F. Xue; Y. R. Shang; X. H. He; J. C. Feng; Z. H. Wu; S. C. Jiang. *Polymer* **2012**, 53, 1593-1601.
31. W. Xu; D. C. Martin; E. M. Arruda. *Polymer* **2005**, 46, 455-470.
32. E. Lezak; Z. Bartczak; A. Galeski. *Polymer* **2006**, 47, 8562-8574.
33. R. Y. Bao; Z. T. Ding; Z.Y. Liu; W. Yang; B. H. Xie; M. B. Yang. *Polymer* **2013**, 54, 1259-1268.
34. A. Pawlak; A. Galeski. *Macromolecules* **2005**, 38, 9688-9697.
35. A. Pawlak; A. Galeski. *Macromolecules* **2008**, 41, 2839-2851.
36. A. Pawlak; A. Galeski. *J. Polym. Sci., Part B: Polym. Phys.* **2010**, 48, 1271-1280.
37. T. Wu; M. Xiang; Y. Cao; J. Kang; F. Yang. *RSC Advances* **2014**, 4, 36689-36701.
38. A. Salazar; P. M. Frontini; J. Rodríguez. *Eng Fract Mech* **2014**, 126, 87-107.
39. C. Z. Geng; G. H. Yang; H. W. Bai; Y. H. Li; Q. Fu; H. Deng. *J Supercrit Fluid* **2014**, 87, 83-92.
40. F. Luo; J. W. Wang; H. W. Bai; K. Wang; H. Deng; Q. Zhang; F. Chen; Q. Fu; B. Na. *Mat Sci Eng A-Struct* **2011**, 528, 7052-7059.
41. H. Liu; J. H. Leng; B. B. He; B. Yang, X. Chen, Q. Q. Qin. *Chin J Polym Sci* **2013**, 31, 1563-1578.
42. C. B. Zhang; G. M. Liu; Y. Song; Y. Zhao; D. J. Wang. *Polymer* **2014**, 55, 6915-6923.
43. A. T. Jones; J. M. Aizlewood; D. R. Beckett. *Makromolekulare Chemie* **1964**, 75, 134-158.
44. J. Varga. *J Therm Anal Calorim* **1986**, 31, 165-172.
45. S. Wang; D. C. Yang. *J Polym Sci Part B: Polym Phys* **2004**, 42, 4320-4325.
46. W. G. Hu; K. Schmidt-Rohr. *Acta Polymerica* **1999**, 50, 271-285.
47. G. Y. Shi; F. Chu; G. E. Zhou; Z. W. Han. *Die Makromol Chem* **1989**, 190, 907-913.
48. B. Lotz; J. C. Wittmann; A. J. Lovinger. *Polymer* **1996**, 37, 4979-4992.
49. Y. M. Mao; C. Burger; X. W. Li; B. S. Hsiao; A. K. Mehta; A. H. Tsou. *Macromolecules* **2011**, 45, 951-961.
50. Y. M. Mao; C. Burger; X. W. Li; B. S. Hsiao; A. K. Mehta; A. H. Tsou. *Polymer* **2013**, 54, 1432-1439.
51. A. Pawlak. *J Appl Polym Sci* **2012**, 125, 4177-4187.
52. B. S. Hsiao; A. D. Kennedy; R. A. Leach; B. Chu; P. Harney. *J Appl Crystallogr* **1997**, 30, 1084-1095.
53. Y. F. Men; J. Rieger; G.Strobl. *Phy Rev Lett* **2003**, 91, 095502.
54. R. Hiss; S. Hobeika; C. Lynn; G. Strobl. *Macromolecules* **1999**, 32, 4390-4403.
55. Y. T. Wang; Z. Y. Jiang; L. L. Fu; Y. Lu; Y. F. Men. *PLoS ONE* **2014**, 9, e97234.
56. A. Pawlak. *Polymer* **2007**, 48, 1397-1409.
57. X. Q. Zhang; K. Schneider; G. M. Liu; J. H. Chen; K. Brüning; D. J. Wang; M. Stamm. *Polymer* **2011**, 52, 4141-4149.
58. A. Galeski. *Prog Polym Sci* **2003**, 28, 1643-1699.
59. Y Y. L. Huang; N. Brown. *J Polym Sci Part B: Polym Phys* **1991**, 29, 129-137.
60. K. H. Nitta; M. Takayanagi. *J Polym Sci Part B: Polym Phys* **1999**, 37, 357-368.
61. K. H. Nitta; H. Nomura. *Polymer* **2014**, 55, 6614-6622.
62. R. Zannetti; G. Celotti; A. Fichera; R. Francesconi. *Die Makromol Chem* **1969**, 128, 137-142.